



저작자표시 2.0 대한민국

이용자는 아래의 조건을 따르는 경우에 한하여 자유롭게

- 이 저작물을 복제, 배포, 전송, 전시, 공연 및 방송할 수 있습니다.
- 이차적 저작물을 작성할 수 있습니다.
- 이 저작물을 영리 목적으로 이용할 수 있습니다.

다음과 같은 조건을 따라야 합니다:



저작자표시. 귀하는 원저작자를 표시하여야 합니다.

- 귀하는, 이 저작물의 재이용이나 배포의 경우, 이 저작물에 적용된 이용허락조건을 명확하게 나타내어야 합니다.
- 저작권자로부터 별도의 허가를 받으면 이러한 조건들은 적용되지 않습니다.

저작권법에 따른 이용자의 권리는 위의 내용에 의하여 영향을 받지 않습니다.

이것은 [이용허락규약\(Legal Code\)](#)을 이해하기 쉽게 요약한 것입니다.

[Disclaimer](#) 

공학석사 학위논문

**Synthesis and Characterization of
Semiconducting Conjugated Polymers
Containing 2,7-Dibenzosilole
for High Open-Circuit Voltage
in Organic Solar Cells**

높은 개방전압의 유기태양전지를 위한
2,7-Dibenzosilole 기반 전도성 고분자의 합성과 특성

2014년 2월

서울대학교 대학원

재료공학부

이강은

Abstract

**Synthesis and Characterization of
Semiconducting Conjugated Polymers
Containing 2,7-Dibenzosilole
for High Open-Circuit Voltage
in Organic Solar Cells**

Lee, KangEun

Materials Science and Engineering

Seoul National University

We synthesized a donor-acceptor (D–A) type conjugated polymer for organic solar cells composed of 2,7-dibenzosilole (DBS) as an electron-rich unit and benzo[c][1,2,5]oxadiazole (BO) as an electron-deficient unit by Suzuki coupling. We also synthesized dithienosilole based D–A type alternating copolymer, PDTSDTBO as reference. The HOMO energy levels of PDBSDTBO and PDTSDTBO were -5.52 eV and -5.23 eV, respectively. The solar cell device fabricated by blending with PDBSDTBO and PC₇₁BM as the active layer has higher V_{OC} than that of the PDTSDTBO-based device, mainly due to the deeper HOMO energy level. The device fabricated with PDBSDTBO and PC₇₁BM exhibits a power conversion efficiency (PCE) of 2.34%, which is higher than that of PDTSDTBO-based device.

Keywords: Benzo[c][1,2,5]oxadiazole, Conjugated polymers, High open circuit voltage, Dibenzosilole, Organic solar cells

Student Number: 2012-22542

Contents

Abstract	i
List of Schemes	iv
List of Figures	v
List of Tables	vii
Chapter 1. Introduction	1
Chapter 2.Experimental Section	5
2.1 Materials	5
2.2 Synthesis of monomers	5
2.3 Synthesis of polymer	16
2.4 Characterization	19
2.5 Device fabrication and measurements	19
Chapter 3.Results and Discussion	23
3.1 Synthesis and Characterization	23
3.2 Optical properties	33
3.3 Electrochemical properties	33
3.4 Photovoltaic properties	38
3.5 Morphology investigation	39
3.6 Charge transport characteristics	40

Chapter 4.Conclusions	46
Bibliography	47
Korean Abstract	51

List of Schemes

Scheme 2.1	The whole synthesis route of monomers	15
Scheme 2.2	The synthetic scheme of polymers	18

List of Figures

Figure 2.1	Polymer Solar cell device structure used in this study	22
Figure 3.1	Chemical structure and ^1H NMR spectrum of 4,4'-Dibromo-2,2'-dinitrobiphenyl	25
Figure 3.2	Chemical structure and ^1H NMR spectrum of 4,4'-Dibromobiphenyl-2,2'-diamine	25
Figure 3.3	Chemical structure and ^1H NMR spectrum of 4,4' -Dibromo-2,2' -diiodobiphenyl	26
Figure 3.4	Chemical structure and ^1H NMR spectrum of 2,7-Dibromo-9,9-dioctyldibenzosilole	26
Figure 3.5	Chemical structure and ^1H NMR spectrum of 9,9-Dioctyl-2,7-bis(4,4,5,5-tetramethyl-1,3,2-dioxaborolane-2-yl)dibenzosilole	27
Figure 3.6	Chemical structure and ^1H NMR spectrum of 3,3' ,5,5' -Tetrabromo-2,2' -bithiophene	27
Figure 3.7	Chemical structure and ^1H NMR spectrum of 3,3' -Dibromo-5,5' -bis(trimethylsilyl)-2,2' -bithiophene	28
Figure 3.8	Chemical structure and ^1H NMR spectrum of 4,4' -Dioctyl-5,5' -bis(trimethylsilyl)dithieno[3,2-b:2' 3' -d]silole	28
Figure 3.9	Chemical structure and ^1H NMR spectrum of 4,4' -Dioctyl-5,5' -dibromodithieno[3,2-b:2' ,3' -d]silole	29
Figure 3.10	Chemical structure and ^1H NMR spectrum of 4,4-Dioctyl-5,5' -bis(trimethyltin)-dithieno[3,2-b:2' ,3' -d]silole	29
Figure 3.11	Chemical structure and ^1H NMR spectrum of 1,2-Bis(octyloxy)benzene	30

Figure 3.12	Chemical structure and ¹ H NMR spectrum of 1,2-Dinitro-4,5-bis(octyloxy)benzene	30
Figure 3.13	Chemical structure and ¹ H NMR spectrum of 5,6-Bis(octyloxy)-4,7-di(thien-2-yl)benzo[c][1,2,5]oxadiazole	31
Figure 3.14	Chemical structure and ¹ H NMR spectrum of 4,7-Dibromo-5,6-bis(octyloxy)benzo[c][1,2,5]oxadiazole	31
Figure 3.15	Chemical structure and ¹ H NMR spectrum of 5,6-Bis(octyloxy)-4,7-di(thien-2-yl)benzo[c][1,2,5]oxadiazole	32
Figure 3.16	Chemical structure and ¹ H NMR spectrum of 4,7-Bis(5-bromothien-2-yl)-5,6-bis(octyloxy)benzo[c][1,2,5]oxadiazole	32
Figure 3.17	UV-Vis absorption spectrum of the polymers as (a) CHCl ₃ solutions and (b) film	35
Figure 3.18	Cyclic voltammograms of the polymers	36
Figure 3.19	Current-voltage (J-V) characteristics of polymer:PC71BM BHJ solar cells under AM 1.5 condition from (a) DCB, (b) DCB with 2 vol% of DIO	41
Figure 3.20	External quantum efficiency spectra of polymer-PCBM solar cells processed with 2 vol% of DIO	43
Figure 3.21	TEM images of polymer:PC ₇₁ BM (1:2, w/w) blend films spin-coated from DCB solution for (a) PDTSDTBO, (b) PDBSDTBO and processed with 2 vol% DIO for (c) PDTSDTBO, (d) PDBSDTBO	44
Figure 3.22	Dark J-V characteristics of polymer : PC ₇₁ BM with hole-only devices with 2 vol% of DIO	45

List of Tables

Table3.1	Summary of optical and electrochemical properties of the polymer.	37
Table 3.2	Photovoltaic properties of devices tested under standard AM 1.5G condition.	42

Chapter 1. Introduction

Availability to all citizens of safe and renewable energy in sufficient quantities is a prerequisite for a sustainable society. A clean energy is necessary to decrease the atmosphere contamination and the greenhouse gas (GHG) emissions to ensure people safety and security. A renewable energy is necessary, meaning that the use of finite fossil resources has to be gradually replaced. Therefore it is necessary to diversify the energy sources, mainly the renewable energies. It is a very urgent goal. Presently almost one thirds of the world population does not have access to electricity, while 20% of the world population of the developed countries use 80% of the world energy production. The very fast increase of the demand of the emerging countries highlights the urgency to develop renewable energies.¹

Currently, the most widely used material for solar cells is inorganic semiconductors such as crystalline silicon. Although the efficiency of the commercial silicon solar cell exceeds over 15%, the fabrication cost is still too expensive to compete with conventional grid electricity without the benefit of government subsidies. To reduce the materials costs, there is a search for inorganic materials for thin film solar cells such as copper-indium-gallium-diselenide (CIGS) or cadmium telluride (CdTe) as the active layer and still provide high efficiencies. However, for these materials abundance of feedstock and issues with toxicity remain the significant problem for worldwide usage.²⁻⁶

Organic solar cells (OSCs) have received much intensively investigated as a promising alternative to silicon based solar cells,^{7,8} due to the low cost, solvent processability and flexibility.^{9,10}

The performance of polymer solar cells has been greatly improved by introduction of bulkheterojunction (BHJ) concept for and active layer. Bulk heterojunction is a blend of the donor and acceptor components in a bulk volume. It exhibits a donor-acceptor phase separation in a 10-20 nm length scale. In such a nanoscale interpenetrating network, each interface is within a distance less than the exciton diffusion length from the absorbing site. The bulk heterojunction concept has heavily increased (orders of magnitude) the interfacial area between the donor and acceptor phases and resulted in improved efficiency of solar cells.¹¹

The BHJ composed of poly(3-hexylthiophene) (P3HT) as the donor and methanofullerene [6,6]-phenyl C61-butyric acid methyl ester (PCBM) as the acceptor was usually employed in OPVs, and the power conversion efficiency (PCE) reached ~5% with optimization.¹²

However, the upper limits of the power conversion efficiency obtained by using PPV or P3HT seem to have been reached due to their relatively high-lying HOMO energy levels, large band gaps and the limited possibilities to alter their electronic properties through structural modification.

Therefore, Donor-Acceptor (D-A) type low-band gap polymers have drawn great attention, as their electronic properties can be easily be changed based on the unique combination of the D-A unit. The principle of the D-A

concept is based on the internal charge transfer (ICT) from an electron donor unit to an electron acceptor unit. The hybridization of the D-A structure leads to a broadening of the valence and conduction bands and thus results in bandgap reduction by raising the HOMO level and lower the LUMO level in conjugated polymer.¹³⁻¹⁶ Therefore, these polymers can also exhibit broader absorption spectra to longer wavelengths compared to more traditional polymers. Along with great efforts on molecular design, device optimization, and device structure innovation, a large amount of D-A type conjugated polymer materials with high power conversion efficiency (PCE) of 6%~8% have been developed.¹⁷⁻²⁰

Especially, silole-containing aromatic units have recently been investigated as novel building blocks for D-A type conjugated polymer materials, because the σ^* -orbital of the silicon-carbon bond can effectively interact with the π^* -orbital of the butadiene fragment, leading to a lowest unoccupied molecular orbital (LUMO) energy level.²¹ Silole-containing conjugated polymers have been widely used in the field of organic light-emitting diodes²² and field-effect transistors (FETs),²³ since they report that 2,5-di(2-pyridyl)silole derivatives exhibit promising electron-transporting properties by Tamao et al.²⁴

Recently, dithieno[3,2-b:2',3'-d]silole (DTS) has often been used as an attractive electron-rich unit of donor-acceptor type conjugated copolymers for polymer solar cells, because it improves the crystallinity²⁵⁻²⁷ and hole mobility²⁴ owing to rigid coplanar structure and the bridging atom of Si instead of C. However, DTS-based polymers have exhibited a

relatively high HOMO energy level due to its strong electron donating ability, causing a low V_{OC} in solar cell devices.²⁸ It is important to obtain high V_{OC} in the devices because the photovoltaic power conversion efficiency of the solar cell is linearly dependent on V_{OC} .

On the other hand, BHJ devices based on main chain D-A polymers containing alkoxy benzoxadiazole (BO) units as acceptors and several thiophene-based building blocks as donors have exhibited relatively high values of V_{OC} ^{29,30}; therefore, combining a strongly electron-withdrawing acceptor with a weakly electron-donating donor can be a very effective means of lowering the HOMO energy level in the D-A polymer and, ultimately, enhancing the value of V_{OC} of the resulting PSC.³¹

In this work, for the purpose to improve the V_{OC} , we introduced 2,7-dibenzosilole (DBS) as an electron-rich unit which has a weaker electron donating ability than DTS, and synthesized a low bandgap polymer (PDBSDTBO) composed of DBS as an electron-rich unit and alkoxy substituted 1,2,5-benzoxadiazole (BO) as an electron-deficient unit. The HOMO energy level of PDBSDTBO (-5.52 eV) is much deeper than that of PDTSDTBO (-5.23 eV), and therefore PDBSDTBO exhibits much higher V_{OC} (0.93 V) of the solar cell device than that of PDTSDTBO (0.72 V).

Chapter 2. Experimental Section

2.1 Materials

All reagents were purchased from Sigma-Aldrich, Alfa-Aesar, TCI chemicals, and Acros Organics and used as received. Tetrahydrofuran (THF) (Daejung Chemicals & Metals) was dried over sodium/benzophenone under nitrogen and freshly distilled before use. Methylene chloride and n-hexane (Daejung Chemicals & Metals) were used without further purification. The chemicals used as solvents for the reactions including polymerization were anhydrous and purchased from the Sigma-Aldrich.

2.2 Synthesis of monomers

2.2.1 Synthesis of 4,4'-Dibromo-2,2'-dinitrophenyl (1)

Scheme 2.1 shows the whole synthesis route of the polymer, PDBSDTBO. To a stirring solution of 2,5-dibromonitrobenzene (24.0 g, 85.4 mmol) in DMF (110 mL) was added copper powder (12.0 g, 188.9 mmol), and the reaction mixture was heated to 125 °C. After 3 h, the mixture was allowed to cool to room temperature. After most of the DMF was evaporated under high vacuum at 60 °C, the mixture was dissolved in benzene (400 mL). The insoluble inorganic salts and excess copper were next removed by filtration through Celite. The filtrate was washed with water and 10% NaHCO₃ and evaporated to dryness. The crude product was next recrystallized from

isopropanol to give 14.9 g (87%) of pure product.

$^1\text{H NMR}$ (300 MHz, CDCl_3): δ 7.17 (d, $J = 8.0$, 2H), 7.84 (dd, $J = 8.0$, 2.0, 2H), 8.39 (d, $J = 2.0$, 2H).

2.2.2 Synthesis of 4,4'-Dibromobiphenyl-2,2'-diamine (2)

To a solution of **1** (11.0 g, 27.4 mmol) in 135 mL of absolute ethanol was added 32 % w/w aqueous HCl (78.0 mL). Tin powder (13.0 g, 108.5 mmol) was then added portionwise over 10 min, and the reaction mixture was heated to reflux at 100 $^\circ\text{C}$ for 2 h. After cooling, the mixture was poured into ice water (400 mL) and then made alkaline with 20% w/w aqueous NaOH solution until the pH was 9.0. The product was next extracted with diethyl ether and the organic layer was washed with brine, dried over anhydrous Na_2SO_4 , filtered, and then evaporated to dryness to give pure product as light-brown crystals that could be used without further purification (8.6 g, 92%).

$^1\text{H NMR}$ (300 MHz, CDCl_3): δ 6.92 (s, 6H), 3.78 (br s, 4H).

2.2.3 Synthesis of 4,4'-Dibromo-2,2'-diiodobiphenyl (3)

A 3-necked flask equipped with a low temperature thermometer was charged with **2** (1.00 g, 2.6 mmol), aqueous HCl (10 mL, 32% w/w), H_2O (40 mL) and acetonitrile (40 mL). The mixture was warmed and stirred until the **2** was dissolved, then cooled to -10 $^\circ\text{C}$, giving a light yellow precipitate. A solution of sodium nitrite (0.92 g, 13.4 mmol) in H_2O (5 mL) was cooled to 0 $^\circ\text{C}$ and added slowly to the reaction mixture, keeping the

reaction temperature between -10 and -5 °C. The reaction was stirred at this temperature for one hour. A solution of KI (4.44 g, 26.7 mmol) in H₂O (10 mL) was cooled to 0 °C and added dropwise via cannula to the reaction mixture with vigorous stirring, whilst maintaining the reaction temperature between -15 °C and -10 °C. Once addition was complete, the reaction was warmed to room temperature and then heated to 80 °C for 20 h. The product was extracted with chloroform (3×100 mL) and the combined organic phases washed with aqueous Na₂S₂O₃ (200 mL), H₂O (200 mL) and brine (200 mL), dried MgSO₄ and evaporated to dryness. Purification by column chromatography on silica gel, using hexane as eluent, followed by recrystallisation from hexane yielded the title compound (0.88 g, 1.56 mmol, 58%) as colorless needles.

¹H NMR (300 MHz, CDCl₃): δ 7.04 (d, J = 8.0, 2H), 7.57 (d, J = 8.0, 2H), 8.11 (s, 2H).

2.2.4 Synthesis of 2,7-Dibromo-9,9-dioctyldibenzosilole (4)

n-Butyllithium (17.0 mL, 42.5 mmol, 2.5 M in hexane) was added portionwise over 2 h to a stirring solution of **3** (6.0 g, 10.64 mmol) in dry THF (120 mL) at -78 °C, under a nitrogen atmosphere. The mixture was next stirred for an additional 1 h at -78 °C. Dichlorodioctylsilane (7.4 mL, 21.37 mmol) was subsequently added and the temperature of the mixture was raised to room temperature and stirred overnight. The reaction mixture was then quenched with distilled water (30.0 mL), and the solvent was removed under vacuum. The product was then dissolved in diethyl ether and

the organic layer washed with brine, dried over anhydrous MgSO_4 , filtered, and evaporated in vacuum giving 8.5 g of crude product as a brownish oil.

Purification by column chromatography (silica gel, hexane) yielded the title compound as a colorless oil (4.2 g, 70%).

^1H NMR (300 MHz, CDCl_3): δ 0.91 (t, 6H), 0.98 (t, 4H), 1.23-1.38 (m, 24H), 7.53 (dd, $J = 8.0, 1.5$, 2H), 7.63 (d, $J = 8.0$, 2H), 7.68 (d, $J = 1.5$, 2H).

2.2.5 Synthesis of 9,9-Dioctyl-2,7-bis(4,4,5,5-tetramethyl-1,3,2-dioxaborolane-2-yl)dibenzosilole (5)

t-Butyllithium (7.77 mL, 13.2 mmol, 1.7 M in pentane) was added over 30 minutes to a solution of **4** (1.78 g, 3.15 mmol) in dry THF (20 mL) at $-78\text{ }^\circ\text{C}$ under nitrogen atmosphere. The mixture was stirred for a further 15 minutes at $-78\text{ }^\circ\text{C}$. 2-Isopropoxy-4,4',5,5'-tetramethyl-1,3,2-dioxaborolane (1.6 mL, 7.87 mmol) was then added dropwise to the mixture and stirring continued overnight at room temperature. The reaction was quenched with distilled water, and THF was removed by vacuum. The product was then extracted into diethyl ether and the organic layer washed with brine, dried with anhydrous MgSO_4 and evaporated. Purification by column chromatography (hexane:ethyl acetate 4:1) yielded the title compound as a white solid (1.64 g, 86 %).

^1H NMR (300 MHz, CDCl_3) δ 0.813 (t, $J = 6.8$, 6H), 0.92-0.96 (m, 4H), 1.18-1.23 (m, 16H), 1.37 (s, 24H), 7.86 (d, $J = 7.0$, 2H), 7.88 (d, $J = 7.0$, 2H), 8.05 (s, 2H).

2.2.6 Synthesis of 3,3',5,5'-Tetrabromo-2,2'-bithiophene (6)

Br₂ (17.8 g, 111 mmol) was added dropwise over 1.5 h to a solution of 2,2'-Bithiophene (5 g, 30 mmol) in glacial AcOH (20 mL) and CHCl₃ (45 mL) at 15 °C. The mixture was stirred at room temperature for 5 h then under reflux for 24 h. After the mixture had been allowed to cool to room temperature, the reaction was quenched by adding aqueous KOH (10%, 50 mL). The aqueous phase was extracted with CHCl₃ (200 mL); the combined extracts were washed with water, dried MgSO₄, filtered, and concentrated under reduced pressure. Recrystallization (EtOH) afforded off-white crystals (66%).

¹H NMR: δ 7.06 (s, 2H).

2.2.6 Synthesis of 3,3'-Dibromo-5,5'-bis(trimethylsilyl)-2,2'-bithiophene (7)

n-BuLi in hexane (1.6M, 25 mL) was added dropwise over a period of 1 h to a solution of **6** (9.56 g, 20.0 mmol) in THF (300 mL) at -78 °C. The mixture was stirred for 15 min, chlorotrimethylsilane (5.4 g, 50 mmol) was added in one portion, and then the cooling bath was removed to warm the mixture to ambient temperature. The volatiles were evaporated under reduced pressure. The residue was purified chromatographically (SiO₂: hexane) to give a colorless oil (1.64 g, 18%).

¹H NMR: δ 7.04 (s, 2H), 0.33 (s, 18H)

2.2.6 Synthesis of 4,4'-Dioctyl-5,5'-bis(trimethylsilyl)dithieno[3,2-b:2',3'-d]silole (8)

n-BuLi in hexane (1.6 M, 4.5 mL) was added dropwise over 5 min to a solution of **7** (1.6 g, 3.4 mmol) in THF (30 mL) at $-78\text{ }^{\circ}\text{C}$. The mixture was stirred for 15 min, dichlorodioctylsilane (1.30 g, 4.00 mmol) was added in one portion, and then the cooling bath was removed, and the mixture was stirred for 2 h under ambient conditions. The mixture was then poured into water and extracted several times with Et_2O . The volatiles were evaporated under a vacuum, and the residue was purified chromatographically (SiO_2 : hexane) to give a colorless oil (0.24 g, 12%).

$^1\text{H NMR}$: δ 7.06 (s, 2H), 1.72 (q, 2H), 1.52-1.14 (m, 16H), 0.92 (t, 6H), 0.86 (t, 6H), 0.76 (m, 4H), 0.32 (s, 18H)

2.2.6 Synthesis of 4,4'-Dioctyl-5,5'-dibromodithieno[3,2-b:2',3'-d]silole (9)

NBS (3.8 g, 21 mmol) was added in one portion to a solution of **8** (5.6 g, 10 mmol) in THF (75 mL). After being stirred at ambient temperature for 4 h, the mixture was extracted with Et_2O , and the volatiles were evaporated under a vacuum. The residue was purified chromatographically (SiO_2 : hexane) to give a yellow oil (5.3 g, 89%).

$^1\text{H NMR}$: δ 6.97 (s, 2H), 1.72 (q, 2H), 1.52-1.14 (m, 16H), 0.92 (t, 6H), 0.86 (t, 6H), 0.76 (m, 4H).

2.2.6 Synthesis of 4,4-Dioctyl-5,5'-bis(trimethyltin)-dithieno[3,2-b:2',3'-d]silole (10)

n-BuLi in hexane (1.6 M, 2.7 mL) was added dropwise to a solution of **9** (1.0 g, 1.7 mmol) in dry THF (30 mL) at -78 °C. After the mixture had been stirred for 15 min, trimethyltin chloride (1.0 g, 5.0 mmol) was added in one portion, and then the cooling bath was removed. The mixture was stirred at ambient temperature for 2 h and then poured into cool water and extracted several times with Et₂O. After evaporation of the volatiles, a sticky pale-green oil was obtained (1.2 g, 92%).

¹H NMR: δ 7.06 (s, 2H), 1.68 (m, 2H), 1.4-1.13 (m, 16H), 0.90 (t, 6H), 0.83 (t, 6H), 0.74 (m, 4H), 0.32 (s, 18H).

2.2.6 Synthesis of 1,2-Bis(octyloxy)benzene (11)

The synthetic route of **11** was synthesized by alkylation of catechol, as shown in Scheme 2.1. A mixture of catechol (10 g, 0.091 mol), 1-bromooctane (40 g, 36 mL, 0.21 mol), and K₂CO₃ (38 g, 0.27 mol) in dry DMF (50 mL) was stirred at 100 °C under a N₂ atmosphere for 40 h. After cooling to room temperature, water (300 mL) was added; the organic layer was separated and the aqueous layer extracted with CH₂Cl₂. The combined organic phases were dried (MgSO₄) and concentrated under reduced pressure. The crude product was purified through column chromatography (SiO₂, hexane) to provide a colorless oil (27 g, 90%).

¹H NMR (300 MHz, CDCl₃): δ 6.89 (s, 2H), 3.99 (t, J = 6.9 Hz, 4H), 1.84-1.77

(m, 4H), 1.49–1.29 (m, 20H), 0.90 (t, J= 6.7Hz, 6H).

2.2.7 Synthesis of 1,2-Dinitro-4,5-bis(octyloxy)benzene (**12**)

65% HNO₃ (20 mL) sample was added dropwise to a two-neck round-bottom flask containing 1,2-bis(octyloxy)benzene (**11**, 10 g, 30 mmol), CH₂Cl₂ (140 mL), and AcOH (140 mL), cooled at 10 °C. The reaction mixture was warmed to room temperature and stirred for 1 h. The mixture was then cooled to 10 °C and 100% HNO₃ (50 mL) was added dropwise. The mixture was warmed to room temperature and stirred for 40 h before being poured into ice-water. The CH₂Cl₂ layer was separated and the aqueous phase extracted with CH₂Cl₂. The organic phases were combined, washed sequentially with water, sat. NaHCO₃(aq), and brine, and then dried (MgSO₄). Concentration under vacuum gave a crude product that was recrystallized from EtOH. Yield: 12 g (95%).

¹H NMR (300 MHz, CDCl₃): δ 7.29 (s, 2H), 4.09 (t, J = 6.6 Hz, 4H), 1.91–1.81 (m, 4H), 1.49–1.28 (m, 20H), 0.89 (t, J= 6.9 Hz, 6H).

2.2.8 Synthesis of 5,6-Bis(octyloxy)benzo[c][1,2,5]oxadiazole (**13**)

A mixture of 1,2-dinitro-4,5-bis(octyloxy)benzene (**12**, 848 mg, 2.00 mmol), NaN₃ (650 mg, 10.0 mmol), and n-Bu₄NBr (130 mg, 0.400 mmol) was heated under reflux in toluene (10 mL) for 12 h. At this point, the starting material had been consumed (TLC); PPh₃ (630 mg, 2.40 mmol) was added and the mixture heated under reflux for an additional 24 h. The reaction mixture was cooled to room temperature and filtered through a short silica plug; the plug was rinsed with CH₂Cl₂. Evaporation of the solvents from

the combined organic phases, under reduced pressure, afforded a crude solid that was recrystallized (EtOH) to yield an off-white solid (683 mg, 63%).
¹H NMR (300 MHz, CDCl₃): δ 6.79 (s, 2H), 4.05 (t, J = 6 Hz, 4H), 1.92–1.83 (m, 4H), 1.54–1.28 (m, 20H), 0.89 (t, J = 6.7 Hz, 6H).

2.2.9 Synthesis of 4,7-Dibromo-5,6-bis(octyloxy)benzo[c][1,2,5]oxadiazole (14)

AcOH (10 mL) and Br₂ (0.850 mL, 16.6 mmol) were added sequentially to a solution of 5,6-bis(octyloxy)benzo[c][1,2,5]oxadiazole (**13**, 1.50 g, 4.00 mmol) in CH₂Cl₂ (80 mL). The resulting mixture was stirred in the dark for 3 days at room temperature and then poured into aqueous NaOH solution (10 g in 200 mL). The aqueous phase was extracted with concentrated under reduced pressure to afford a crude solid that was CH₂Cl₂; the combined organic extracts were washed with brine and purified through column chromatography [SiO₂, hexane/CH₂Cl₂, 9:1 (v/v)] to yield a white solid (2.2 g, 79%).

¹H NMR (300 MHz, CDCl₃): δ 4.13 (t, J = 9 Hz, 4H), 1.89–1.80 (m, 4H), 1.53–1.29 (m, 20H), 0.88 (t, J = 6.6 Hz, 6H)

2.2.10 Synthesis of 5,6-Bis(octyloxy)-4,7-di(thien-2-yl)benzo[c][1,2,5]oxadiazole (15)

Tributylstannylthiophene (994 μL, 3.13 mmol) was added to a solution of 4,7-dibromo-5,6-bis(octyloxy)benzo[c][1,2,5]oxadiazole (**14**, 665 mg, 1.25 mmol), tris(dibenzylideneacetone)dipalladium (Pd₂(dba)₃; 46 mg, 0.050 mmol), and tri-*o*-tolylphosphine (122 mg, 0.400 mmol) in dry toluene (10 mL) and then the reaction mixture was heated under reflux for 16 h under N₂. The reaction

mixture was concentrated directly under vacuum. Dry column chromatography [SiO₂, hexane/CHCl₃, 10:1 (v/v)] afforded a yellow solid (470mg, 70%).

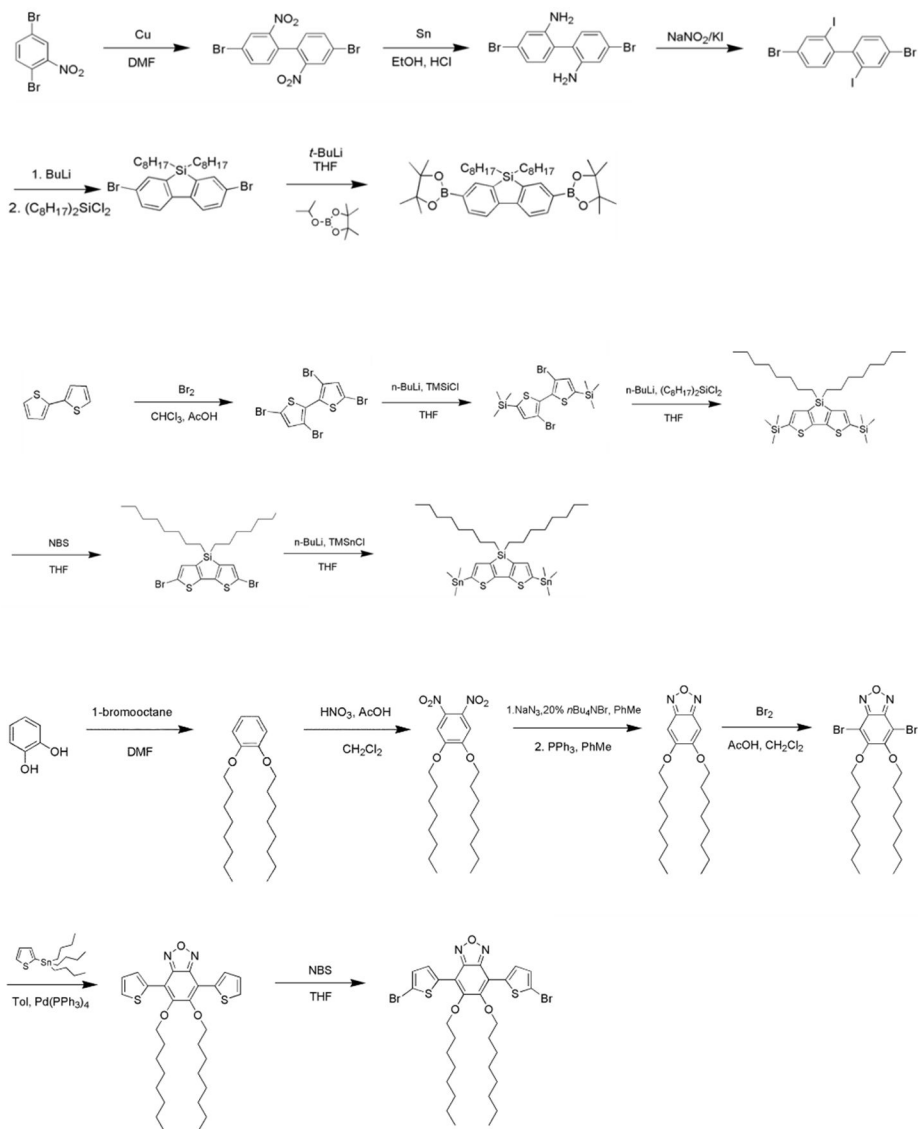
¹H NMR (300MHz, CDCl₃): δ 8.46 (d, J = 3.6 Hz, 2H), 7.50 (d, J = 6.3 Hz, 2H), 7.22 (t, J = 4.5 Hz, 2H), 4.14 (t, J = 7.2 Hz, 4H), 2.051.95 (m, 4H), 1.471.30 (m, 20H), 0.90 (t, J = 3.3 Hz, 6H).

2.2.11 Synthesis of 4,7-Bis(5-bromothien-2-yl)-5,6-bis(octyloxy)benzo[c][1,2,5]oxadiazole (16)

NBS (355 mg, 2.00 mmol) was added in one portion to a solution of **15** (540 mg, 1.00 mmol) in CHCl₃ (40 mL), and glacial AcOH (40 mL) and then the mixture was stirred at room temperature for 20 h in the dark. The solution was concentrated directly onto celite under vacuum. Dry column chromatography [SiO₂, hexane/CHCl₃, 9:1 (v/v)] afforded an orange solid (800 mg, 92%).

¹H NMR (300 MHz, CDCl₃): δ 8.22 (d, J = 4.2 Hz, 2H), 7.15 (d, J = 4.5 Hz, 2H), 4.14 (t, J = 7.5 Hz, 4H), 2.041.94 (m, 4H), 1.471.30 (m, 20H), 0.90 (t, J = 2.4 Hz, 6H).

¹³C NMR (500MHz, CDCl₃): δ 151.1, 146.1, 134.2, 131.1, 130.0, 116.3, 112.6, 74.7, 31.7, 30.1, 29.4, 29.2, 25.7, 22.6, 14.1.



Scheme 2.1 The whole synthesis route of monomers

2.3 Synthesis of polymers

2.3.1 Synthesis of PDBSDTBO

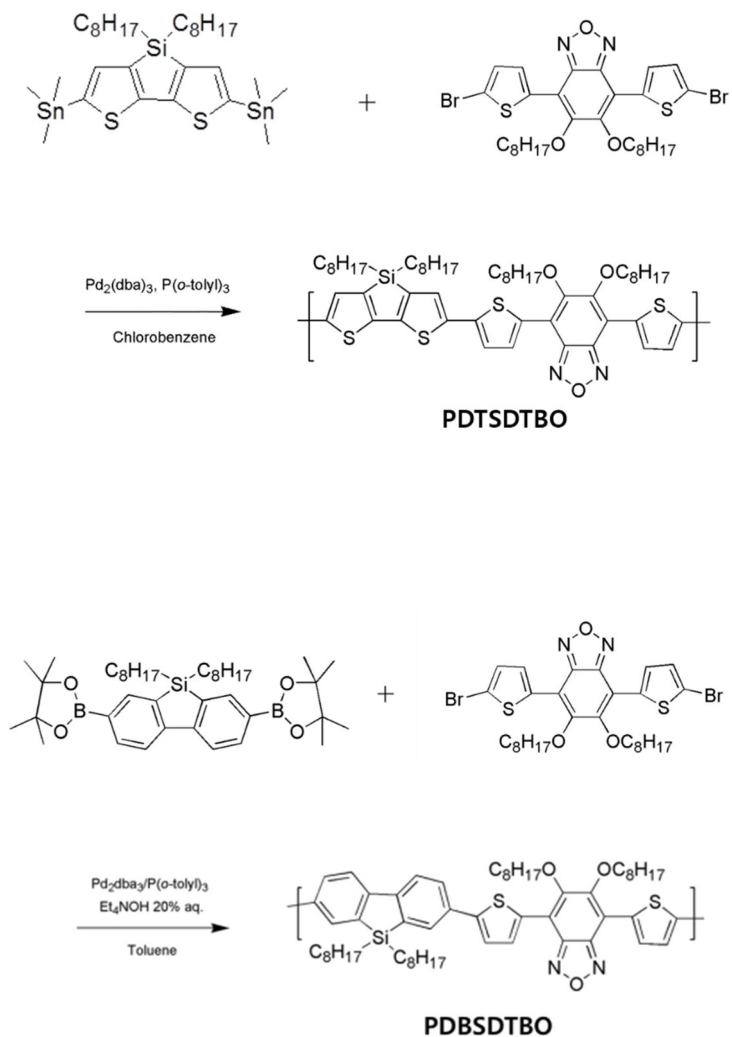
9,9-Dioctyl-2,7-bis(4,4,5,5-tetramethyl-1,3,2-dioxaborolane-2-yl) dibenzosilole (**5**, 100mg, 0.152 mmol) and 4,7-Bis(5-bromothien-2-yl)-5,6-bis(octyloxy)benzo[*c*][1,2,5]oxadiazole (**16**, 106 mg, 0.152 mmol) were dissolved in a mixture of toluene (10 ml) and aqueous K₃PO₄ solution (2M, 1.5 ml). The solution was flushed with Ar for 20min, and then Tris(dibenzylideneacetone)dipalladium (10 mg, 11 μmol), tri(*o*-tolyl)phosphine (9.2mg, 0.03 mmol) and Aliquat336 (2drops) were added.

This mixture was stirred for 2 hours at 150 °C in microwave reactor after which the crude polymer was precipitated in methanol. The precipitate was collected in a soxhlet thimble and was extracted with methanol, acetone, ethyl acetate, hexane, and chloroform until the extracts were colorless. The chloroform fraction was reduced in volume and precipitated in methanol and filtered over a 4.5 μm PTFE filter. The polymer was collected and dried in a vacuum oven at 40 °C overnight, resulting in 77 mg (54%) of a dark red powder. M_n= 13200 g mol⁻¹ (polydispersity index 1.24)

2.3.2 Synthesis of PDTSDTBO

4,4-Dioctyl-5,5'-bis(trimethyltin)-dithieno[3,2-*b*:2',3'-*d*]silole (**10**, 100mg, 0.134 mmol) and 4,7-Bis(5-bromothien-2-yl)-5,6-bis(octyloxy)benzo[*c*][1,2,5]oxadiazole (**16**, 93.8 mg, 0.134 mmol) were dissolved in a mixture of chlorobenzene (10 ml). The solution was flushed with Ar for 20min, and then Tris(dibenzylideneacetone)dipalladium (10 mg, 11 μmol), tri(*o*-tolyl)phosphine (9.2mg, 0.03 mmol) were added. This mixture

was stirred for 2 hours at 150 °C in microwave reactor after which the crude polymer was precipitated in methanol. The precipitate was collected in a soxhlet thimble and was extracted with methanol, acetone, ethyl acetate, hexane, and chloroform until the extracts were colorless. The chloroform fraction was reduced in volume and precipitated in methanol and filtered over a 4.5 µm PTFE filter. The polymer was collected and dried in a vacuum oven at 40 °C overnight, resulting in 60 mg (47%) of a dark purple powder. $M_n = 11200 \text{ g mol}^{-1}$ (polydispersity index 1.04)



Scheme 2.2 The synthetic scheme of polymers

2.4 Characterization

The chemical structures of the materials used in this study were identified by

^1H NMR (Avance DPX-300) and ^{13}C NMR (Avance DPX-500). Molecular weight and its distribution were measured by gel permeation chromatography (Waters) equipped with a Waters 2414 refractive index detector using CHCl_3 as an eluent, where the columns were calibrated against standard polystyrene samples. The optical absorption spectra were obtained by a UV-Vis spectrophotometer (Lambda 25, Perkin Elmer). Cyclic voltammetry experiments were carried out on a potentiostat/galvanostat (VMP 3, Biologic) in an electrolyte solution of 0.1 M tetrabutylammonium hexafluorophosphate (Bu_4NPF_6) in Acetonitrile. Platinum wires (Bioanalytical System Inc.) were used as both counter and working electrodes, and silver/silver ion (Ag in 0.1M AgNO_3 solution, Bioanalytical System Inc.) was used as a reference electrode. The HOMO energy level of the polymers were calculated using the equation: $\text{HOMO} = - [\text{E}_{\text{ox}} - \text{E}_{1/2}(\text{ferrocene}) + 4.8] \text{ V}$, where E_{ox} is the onset oxidation potential of the polymer and $\text{E}_{1/2}(\text{ferrocene})$ is the onset oxidation potential of ferrocene vs. Ag/Ag^+ . The samples for transmission electron microscopy (TEM) were prepared by floating a film in water and put on a 300 mesh Cu grid. TEM observation was performed on a JEM 1010 microscope with an accelerating voltage of 80 kV.

2.5 Device fabrication and measurements

2.5.1. Materials

ITO-patterned glass was used as an anode in PSC device. The sheet resistance of the ITO was less than 10 Ω /square. PC_{71}BM (>99.5%) was obtained from

Nano-C. These chemicals were used as received without further purification. Poly(3,4-ethylenedioxythiophene):poly(styrene sulfonate) (PEDOT:PSS) (Baytron PVP Al 4083) was purchased from H. C. Stark and passed through a 0.2 μm PTFE syringe filter before spin coating.

2.5.2.Solar cell device fabrication

Polymer solar cells were fabricated on ITO glass cleaned by stepwise sonication in acetone and IPA, followed by O_2 plasma treatment for 10 min. PEDOT:PSS was spin-coated on the ITO glass at 4000rpm for 1 min and annealed at 140 $^\circ\text{C}$ for 20 min to yield a 40 nm thick film. A mixture of polymer and PC_{71}BM were dissolved in anhydrous *o*-dichlorobenzene (20 mg ml⁻¹), and spin-coated on the top of the ITO-PEDOT:PSS film at 800 rpm for 60 s. The typical thickness of the active layer was 80 nm. Calcium (20 nm) and aluminum (100 nm) were evaporated, under a vacuum lower than 10^{-6} Torr, on the top of the active layer through a shadow mask. The effective area of the cell was ca. 4mm².

2.5.3.Solar cell performance measurements.

The photovoltaic performance was measured under nitrogen atmosphere inside the glove box. The current density-voltage (J-V) characteristics were measured with a Keithley 4200 source-meter under AM 1.5 G (100mW/cm²) simulated by a Newport-Oriel solar simulator. The light intensity was calibrated using a NREL certified photodiode and light source meter prior to each measurement. The active area was determined at 4mm² by attaching a

shadow mask onto solar cell device. The external quantum efficiency (EQE) was measured using a Polaronix K3100 IPCE measurement system (McScience). The light intensity at each wavelength was calibrated with a standard single-crystal Si cell.

For hole mobility measurements, hole-only devices were fabricated having the structure ITO/PEDOT:PSS/polymer/Au. The hole mobility was determined by fitting the dark J-V curve into the space-charge-limited current

method^{32,33} based on the equation,

$$J = (9/8)\epsilon_r\epsilon_0\mu_h(V^2/L^3)$$

where ϵ_0 is the permittivity of free space, ϵ_r is the dielectric constant of the polymer which is assumed to be around 3 for the conjugated polymers, μ_h is the hole mobility, V is the voltage drop across the device, and L is the thickness of active layer. The data was measured with a Keithley 4200 source-meter under AM 1.5 G (100mW/cm²) simulated by a Newport-Oriel solar simulator. To obtain μ_h , the equation is changed to $J^{1/2} = (9/8)^{1/2}\epsilon_r^{1/2}\epsilon_0^{1/2}\mu_h(V/L^{3/2})$. L is obtained by atomic force microscopy (AFM). Then, the hole mobility would be calculated from the slope of the plotted data.

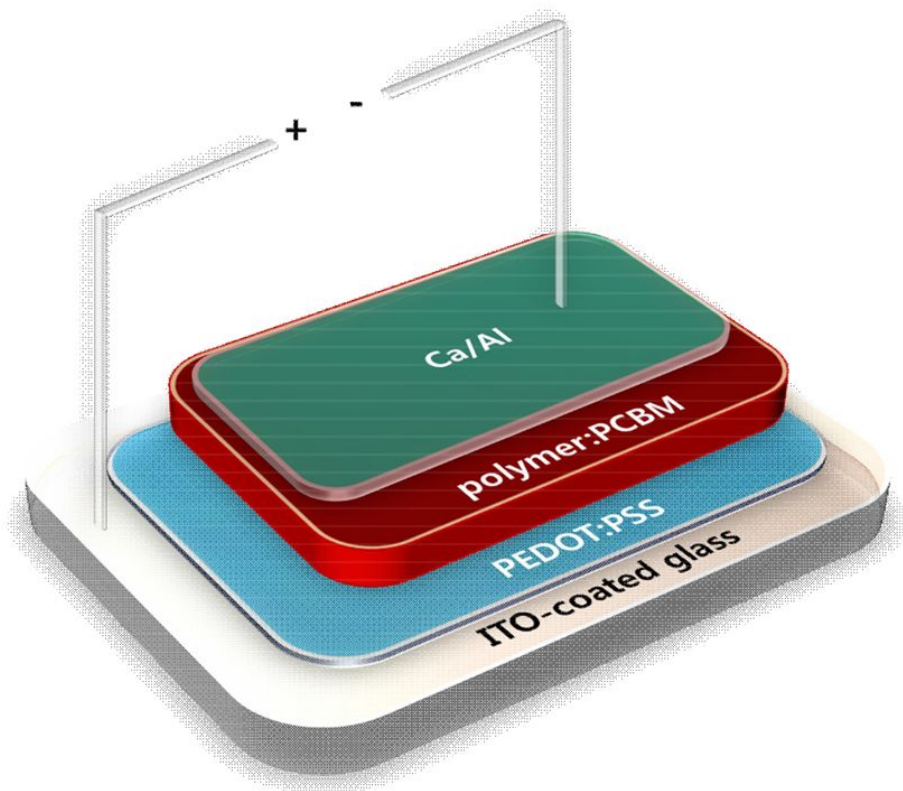


Figure2.1 Polymer Solar cell device structure used in this study.

Chapter 3. Results and Discussion

3.1 Synthesis and Characterization

The chemical structures of 4,4'-Dibromo-2,2'-dinitrobiphenyl(1), 4,4'-Dibromobiphenyl-2,2'-diamine(2), 4,4' -Dibromo-2,2' -diiodobiphenyl(3), 2,7-Dibromo-9,9-dioctyldibenzosilole (4),9,9-Dioctyl-2,7-bis(4,4,5,5-tetramethyl-1,3,2-dioxaborolane-2-yl)dibenzosilole (5), 3,3' ,5,5' -Tetrabromo-2,2' -bithiophene (6), 3,3' -Dibromo-5,5' -bis(trimethylsilyl)-2,2' -bithiophene (7),4,4' -Dioctyl-5,5' -bis(trimethylsilyl)dithieno[3,2-b:2' 3' -d]silole (8), 4,4' -Dioctyl-5,5' -dibromodithieno[3,2-b:2' ,3' -d]silole (9), 4,4-Dioctyl-5,5' -bis(trimethyltin)-dithieno[3,2-b:2' ,3' -d]silole (10), 1,2-Bis(octyloxy)benzene (11), 1,2-Dinitro-4,5-bis(octyloxy)benzene (12), 5,6-Bis(octyloxy)benzo[c][1,2,5]oxadiazole (13), 4,7-Dibromo-5,6-bis(octyloxy)benzo[c][1,2,5]oxadiazole (14), 5,6-Bis(octyloxy)-4,7-di(thien-2-yl)benzo[c][1,2,5]oxadiazole (15)and 4,7-Bis(5-bromothien-2-yl)-5,6-bis(octyloxy)benzo[c][1,2,5]oxadiazole(16) are identified by ¹H NMR, as shown in Figure 3.1-16, respectively.

The synthesis scheme of monomer **16** has been largely investigated because it is a promising building block for donormaterials used in PSCs, which exhibit higher PCE. In practice, because of their limited solubility, many benzooxadiazole-based polymers are of lower molecular weight. The introduction of two flexible alkoxy chains onto the benzooxadiazole can

significantly increase the solubility of polymers without drastically decreasing the planarity of polymer main chains and without significant influence on their energy levels. Other advantage of the alkoxy-modified benzoxadiazole is that it can be synthesized easily because the product is obtained by recrystallization in methanol as the solid forms of needle or powder.

However, monomer **5** (dibenzosilole) and monomer **10** (dithienosilole) are obtained as liquid without recrystallization, implying low quality of purity. The impurity of the monomer for polymerization causes low molecular weight of the polymer which is not suitable for the polymer solar cell device. High molecular weight of the polymer is desirable for the PSCs because long chain is beneficial for forming the nanoscale morphology of interpenetrating network inducing high hole mobility. For instance, the molecular weight of rr-P3HT has a significant impact on the resulting film morphology and hole mobility. High-molecular-weight rr-P3HT has demonstrated three orders of magnitude improvement in hole mobility, and a much enhanced OPV cell efficiency.³⁴ As a result of the impurity of monomer **5** and **10**, the resulting polymers, PDBSDTBO and PDTSDTBO had low molecular weight compared to the conventional semiconducting conjugated polymers for polymer solar cells. The number-average molecular weight of PDBSDTBO was 13200 g mol⁻¹ (polydispersity index 1.24) and, that of PDTSDTBO was 11200 g mol⁻¹ (polydispersity index 1.04). Therefore, further synthesis method would be needed for monomer **5** and **10**.

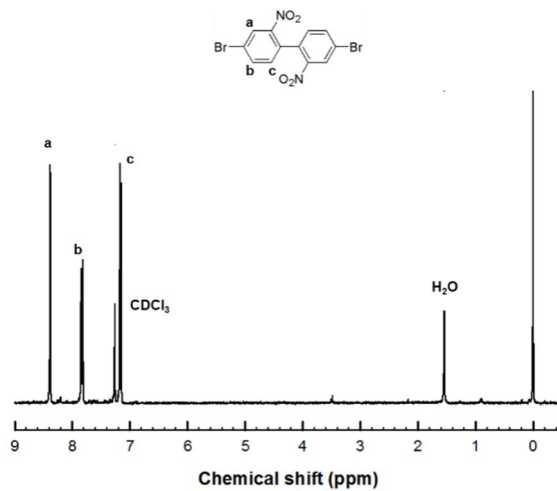


Figure3.1 Chemical structure and ^1H NMR spectrum of 4,4'-Dibromo-2,2'-dinitrobiphenyl

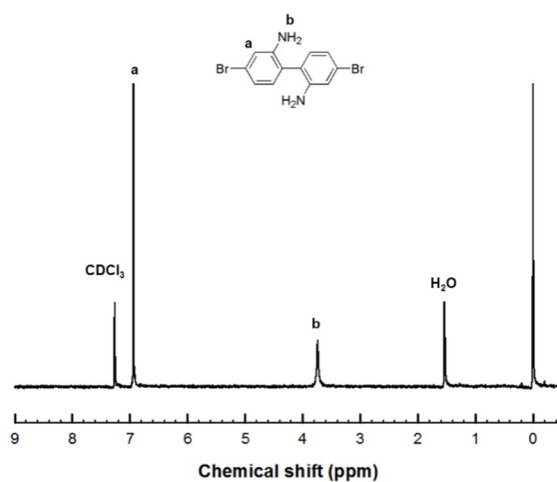


Figure3.2 Chemical structure and ^1H NMR spectrum of 4,4'-Dibromobiphenyl-2,2'-diamine

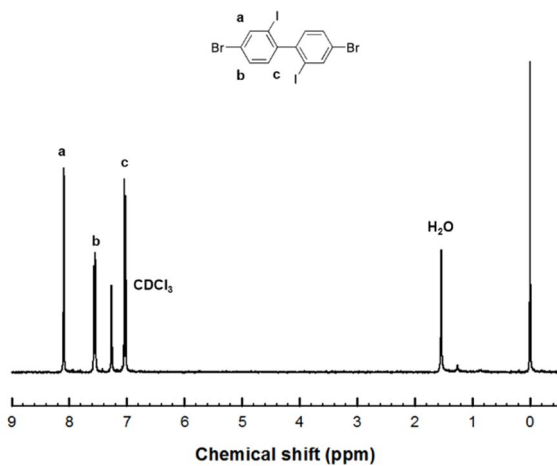


Figure3.3 Chemical structure and ^1H NMR spectrum of
4,4' -Dibromo-2,2' -diiodobiphenyl

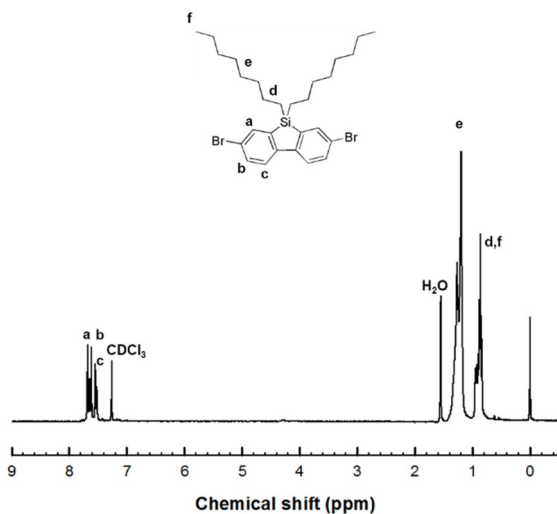


Figure3.4 Chemical structure and ^1H NMR spectrum of
2,7-Dibromo-9,9-dioctyldibenzosilole

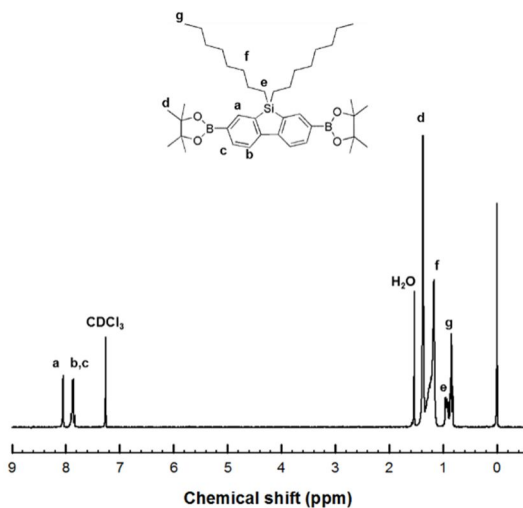


Figure 3.5 Chemical structure and ^1H NMR spectrum of 9,9-Dioctyl-2,7-bis(4,4,5,5-tetramethyl-1,3,2-dioxaborolane-2-yl)dibenzosilole

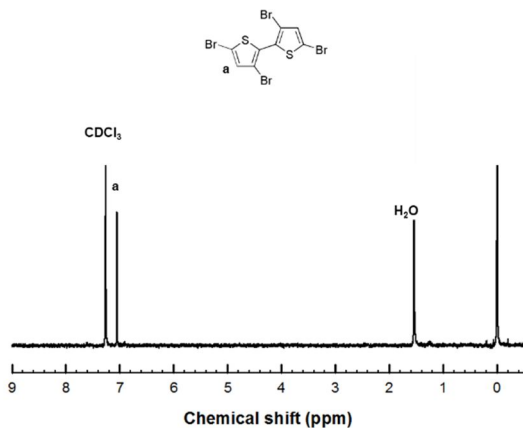


Figure 3.6 Chemical structure and ^1H NMR spectrum of 3,3',5,5'-Tetrabromo-2,2'-bithiophene

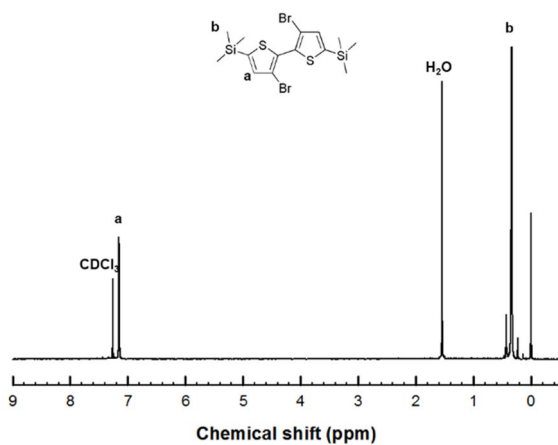


Figure3.7 Chemical structure and ^1H NMR spectrum of 3,3'-Dibromo-5,5'-bis(trimethylsilyl)-2,2'-bithiophene

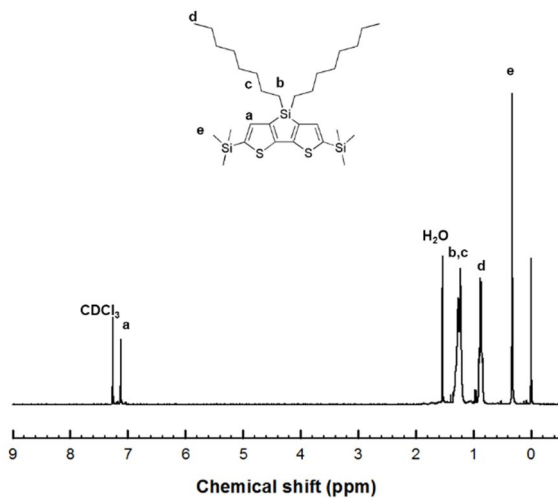


Figure3.8 Chemical structure and ^1H NMR spectrum of 4,4'-Dioctyl-5,5'-bis(trimethylsilyl)dithieno[3,2-b:2' 3'-d]silole

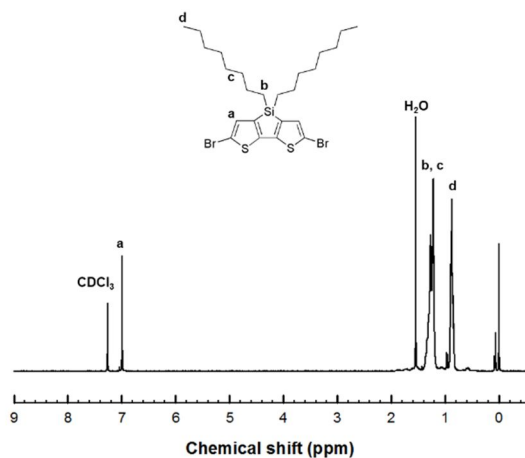


Figure3.9 Chemical structure and ¹H NMR spectrum of 4,4'-Dioctyl-5,5'-dibromodithieno[3,2-b:2',3'-d]silole

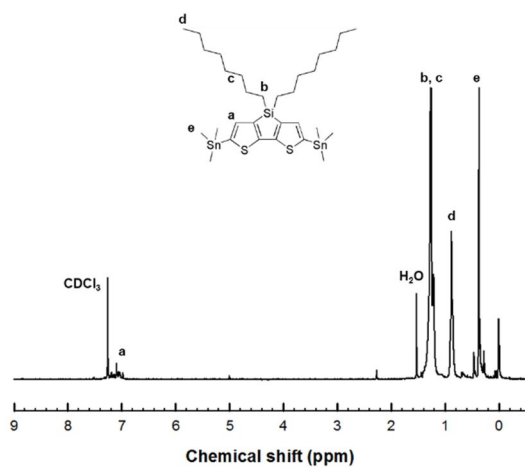


Figure3.10 Chemical structure and ¹H NMR spectrum of 4,4'-Dioctyl-5,5'-bis(trimethyltin)-dithieno[3,2-b:2',3'-d]silole

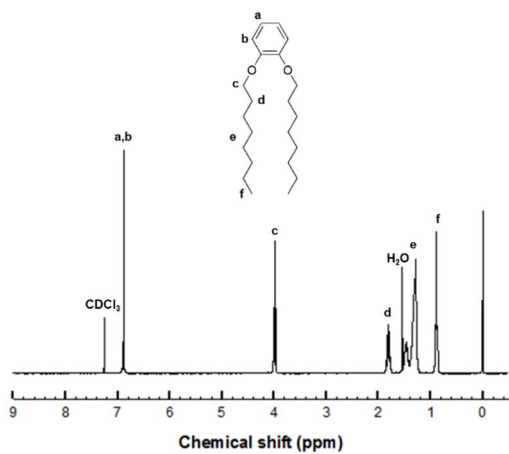


Figure3.11 Chemical structure and ^1H NMR spectrum of 1,2-Bis(octyloxy)benzene

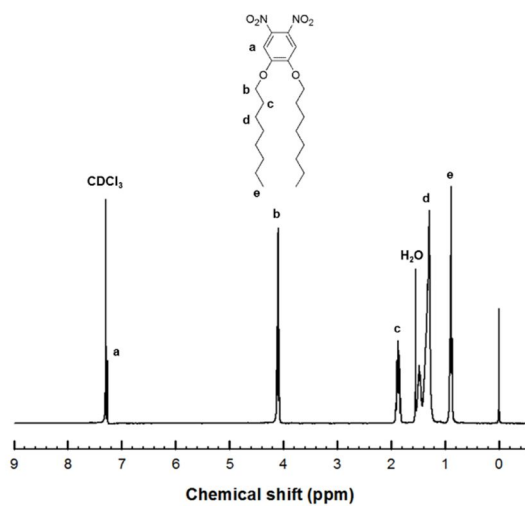


Figure3.12 Chemical structure and ^1H NMR spectrum of 1,2-Dinitro-4,5-bis(octyloxy)benzene

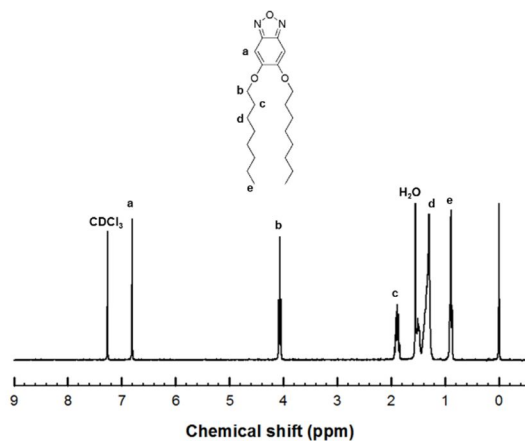


Figure3.13 Chemical structure and ^1H NMR spectrum of 5,6-Bis(octyloxy)benzo[c][1,2,5]oxadiazole

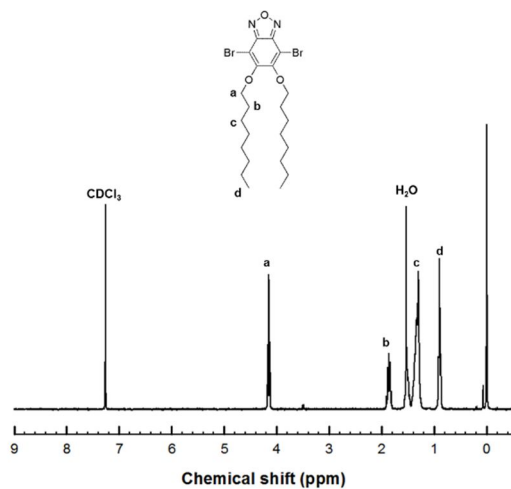


Figure3.14 Chemical structure and ^1H NMR spectrum of 4,7-Dibromo-5,6-bis(octyloxy)benzo[c][1,2,5]oxadiazole

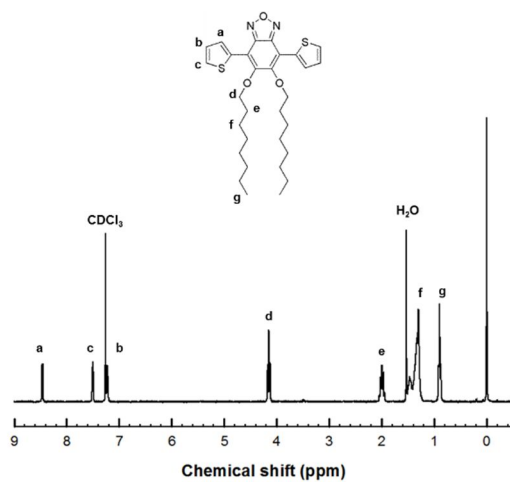


Figure3.15 Chemical structure and ^1H NMR spectrum of 5,6-Bis(octyloxy)-4,7-di(thien-2-yl)benzo[c][1,2,5]oxadiazole

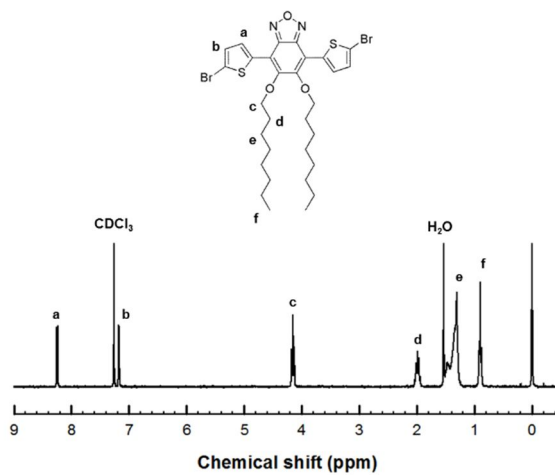


Figure3.16 Chemical structure and ^1H NMR spectrum of 4,7-Bis(5-bromothien-2-yl)-5,6-bis(octyloxy)benzo[c][1,2,5]oxadiazole

3.2 Optical properties

We recorded the optical UV-Vis absorption spectra of the PDTSDTBO and PDBSDTBO from their dilute CHCl_3 solutions at room temperature and as spin-coated films on quartz substrates (Figure 3.12). Table 3.1 summarizes the optical data, including the absorption peak wavelengths (λ_{max}), and the optical band gap ($E_{\text{g}}^{\text{opt}}$). $E_{\text{g}}^{\text{opt}}$ is obtained by the absorption edge wavelengths of the films for PDTSDTBO and PDBSDTBO corresponding to 738 nm and 660 nm, respectively. In Figure 3.12, PDTSDTBO and PDBSDTBO displayed quite similar absorption spectra both in solutions and films. All of the absorption spectra appear as two absorption bands: one at 300–420 nm, which we assign to localized $\pi-\pi^*$ transitions, and another, broader band from 420 to 700 nm in the long wavelength region, corresponding to intramolecular charge transfer (ICT) between the acceptor (BO) and donor units.^{35,36} PDBSDTBO had slightly more light absorption in short wavelength region, however, the absorption spectra of PDTSDTBO in both solution and film were slightly broader and red-shifted than those of PDBSDTBO. Thus, the amounts of light absorption of the two polymers were almost the same. The absorption spectra of the two polymers in the solid state were similar to their corresponding solution spectra, with slight red-shifts (ca. 5–40 nm) of their absorption maxima, indicating that some intermolecular interactions existed in the solid state.

3.3 Electrochemical properties

The electrochemical data of all the polymers are obtained from the

oxidation and reduction cyclic voltammograms, as shown in Figure 3.13 and are summarized in Table 3.1. The HOMO energy level of the polymers were calculated using the equation: $\text{HOMO} = -[E_{\text{ox}} - E_{1/2}(\text{ferrocene}) + 4.8] \text{ V}$, where E_{ox} is the onset oxidation potential of the polymer and $E_{1/2}(\text{ferrocene})$ is the onset oxidation potential of ferrocene vs. Ag/Ag^+ . Since the open circuit voltage (V_{OC}) of polymer solar cells is linearly dependent on the difference between the HOMO energy level of the electron donor and the LUMO energy level of the electron acceptor³⁷, the deep HOMO energy level of the donor polymer is expected to afford a high V_{OC} for the resulting polymer solar cells. PDBSDTBO has deep HOMO energy level (-5.52 eV), which is relatively lower than that of PDTSDTBO (-5.23 eV). The LUMO energy levels of the polymers were calculated using the equation: $\text{LUMO} = -[E_{\text{red}} - E_{1/2}(\text{ferrocene}) + 4.8] \text{ V}$, where E_{red} is the onset reduction potential of the polymer. The LUMO energy level of PDBSDTBO and PDTSDTBO were -3.60 eV and -3.58 eV, respectively. The energy band gap calculated from the electrochemical properties of PDBSDTBO and PDTSDTBO were 1.92 eV and 1.65 eV, respectively which are different from the optical band gap. Indeed, the value of the LUMO energy level of polymers from the cyclic voltammogram is not correct. Thus, the optical band gap of polymers are used instead of electrochemical band gap. Considering that a LUMO-LUMO offset of 0.3-0.4 eV is necessary for efficient electron transfer from donor polymer to PCBM³⁸, it is expected that excitons can be easily dissociated at the interface between PDBSDTBO and PCBM, because the LUMO energy level (-3.64 eV) of the polymer is sufficiently higher than that of PCBM (-4.0 eV).

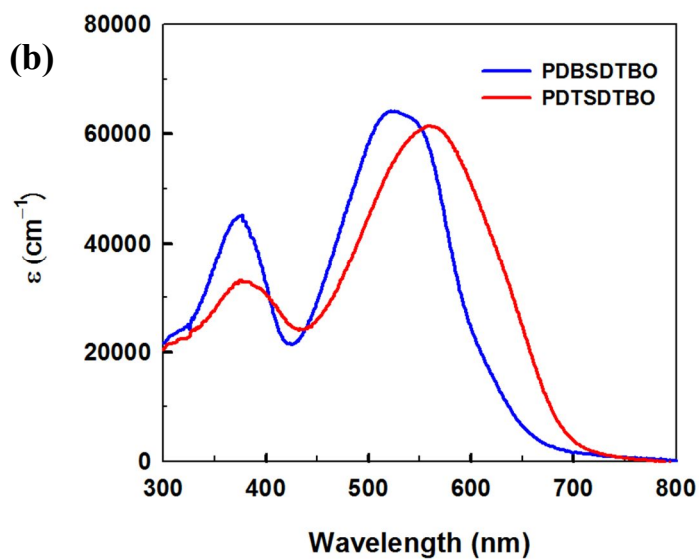
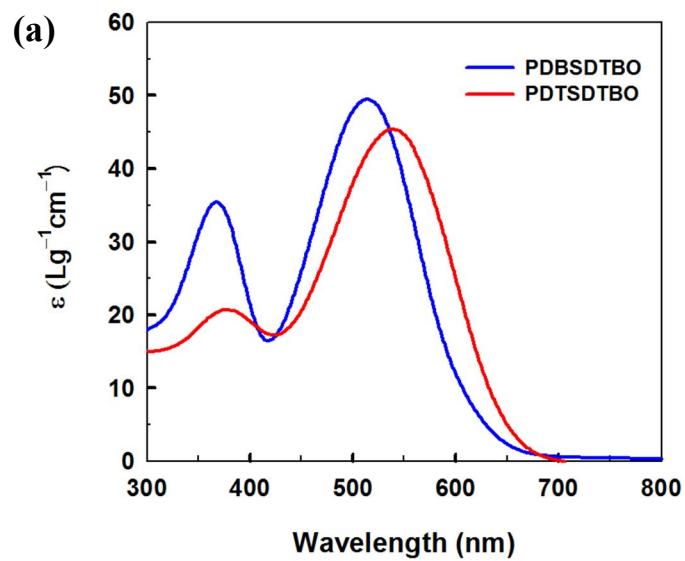


Figure3.17 UV-Vis absorption spectrum of the polymers as (a) CHCl_3 solutions and (b) film.

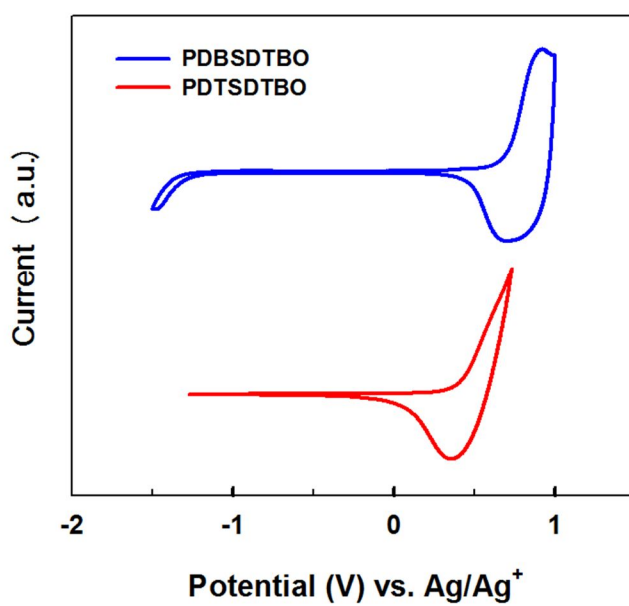


Figure 3.18 Cyclic voltammograms of the polymers

Table 3.1 Summary of optical and electrochemical properties of the polymer.

Polymer	M_n (kg/mol)	PDI	λ_{\max} (nm)		E_g^{opt} (eV)	HOMO (eV)	LUMO ^a (eV)
			Solution	Film			
PDTSDTBO	11.2	1.04	367, 513	375, 555	1.68	-5.23	-3.55
PDBSDTBO	13.2	1.24	376, 538	373, 520	1.88	-5.52	-3.64

^aCalculated from $E_{\text{LUMO}} = E_{\text{HOMO}} + E_g^{\text{opt}}$

3.4 Photovoltaic properties

The polymer solar cells were fabricated with a layered configuration of ITO/PEDOT:PSS/polymer:PC₇₁BM/Ca/Al. The J-V characteristics of photovoltaic devices prepared from polymer:PC₇₁BM using 1,2-dichlorobenzene as a processing solvent are represented in Figure 3.14 (a), and their photovoltaic properties are summarized in Table 3.2. To optimize the performance of OPVs, 2 vol% of 1,8-diiodooctane (DIO) was added into the solution of polymers and PC₇₁BM as a processing additive represented in Figure 3.14 (b). It has recently been reported that the morphology of active layer can be effectively modified and optimized by the use of DIO. Compared with Figure 3.14 (a) and (b), the devices processed with 2 vol% of DIO showed the higher values of J_{SC} and FF than those fabricated with no additive for both PDBSDTBO and PDTSDTBO. The optimized weight ratio for the polymer and PC₇₁BM was 1:2. The higher PCE of the PDBSDTBO-based device than that of the PDTSDTBO-based device is attributed to V_{OC}, J_{SC} and FF. It should be noted here that the V_{OC} of PDBSDTBO-based device (0.93 V) is higher than that of PDTSDTBO-based device (0.72 V), which is in accordance with the deeper HOMO level of the PDBSDTBO than that of PDTSDTBO.

The short-circuit current densities (J_{SC}) of the devices incorporating PDTSDTBO and PDBSDTBO processed with 2 vol% of DIO were 3.17 and 4.93 mA cm⁻², respectively. Figure 3.15 shows the EQE curves of the devices based on the polymer/PC₇₁BM blends at weight ratios of 1:2 processed with 2 vol% of DIO. The theoretical J_{SC} obtained from integrating the EQE curves of

the PDTSDTBO and PDBSDTBO blends were 2.98 and 4.76 mA cm⁻²— values that agree reasonably with the measured (AM 1.5G) values of J_{SC}, with discrepancies of less than 5%.

3.5 Morphology investigation

When exploring the decisive factors affecting the efficiencies of PSCs, we must consider not only the absorption and energy levels of the polymers but also the morphologies of the polymer blends.³⁹ Figure 3.16 shows TEM images of the polymer/PC₇₁BM blend films. We prepared samples of the polymer/PC₇₁BM blends using procedures identical to those employed to fabricate the active layers of the devices. In Figure 3.16, as the electron scattering density of PCBM was higher than that of the conjugated polymer, the polymer domains appear as bright regions; the dark regions are attributed to PC₇₁BM domains. Figure 3.16 (a) and (b) shows the island-shaped features of the aggregated PC₇₁BM domains (dark areas) in the blend films processed without additives. In contrast, Figure 3.16 (c) and (d) shows the homogeneous morphologies of the polymer/PC₇₁BM blend films processed with 2 vol% of DIO as additives, indicating that the incorporation of the additives optimized the miscibility of the polymer chains with PC₇₁BM. However, Figure 3.16(c) shows the microscale of phase segregation which is not suitable for BHJ concept in the blend film with PDTSDTBO/PC₇₁BM causing the charge recombination inducing low value of the J_{SC} of PDTSDTBO based device. In contrast, Figure 3.16 (d) shows the nanoscale phase segregation of the PDBSDTBO/PC₇₁BM blend

which is suitable for exciton dissociation and charge transport leading to its devices exhibiting greater photocurrents.

3.6 Charge transport characteristics

The higher FF for the PDBSDTBO-based device was likely due to the higher hole mobility of this active layer (Figure 3.17). It is known that unbalanced charge mobility increases the built-up of space charges and charge recombinations causing low FF.⁴⁰ Therefore, high hole mobility of the p-type conjugated polymer is needed to balance with the electron mobility of the PC₇₁BM ($2 \times 10^{-7} \text{ cm}^2 \text{ V}^{-1} \text{ s}^{-1}$). The hole mobility was measured from the space charge limited current (SCLC) J-V curves as obtained in the dark using hole-only devices (ITO/PEDOT:PSS/polymer:PC₇₁BM/Au). The SCLC behavior is analyzed using the Mott-Gurney law: $J = (9/8)\epsilon\mu(V^2L^{-3})^{41}$, where ϵ is the static dielectric constant of the medium, μ is the charge carrier mobility, $V = V_a - V_{bi}$ (V_a , the applied bias; V_{bi} , the built-in potential due to the difference in electrical contact work functions), and L is the layer thickness. The mobility is obtained from the slope of the plot of $J^{1/2}$ vs. V (Figure 3.13). Indeed, the hole mobility of PDBSDTBO/PCBM blend ($9.13 \times 10^{-6} \text{ cm}^2 \text{ V}^{-1} \text{ s}^{-1}$) is much higher than that of PDTSDTBO/PCBM blend ($3.7 \times 10^{-7} \text{ cm}^2 \text{ V}^{-1} \text{ s}^{-1}$) inducing higher FF of the PDBSDTBO based device than that of the PDTSDTBO based device.

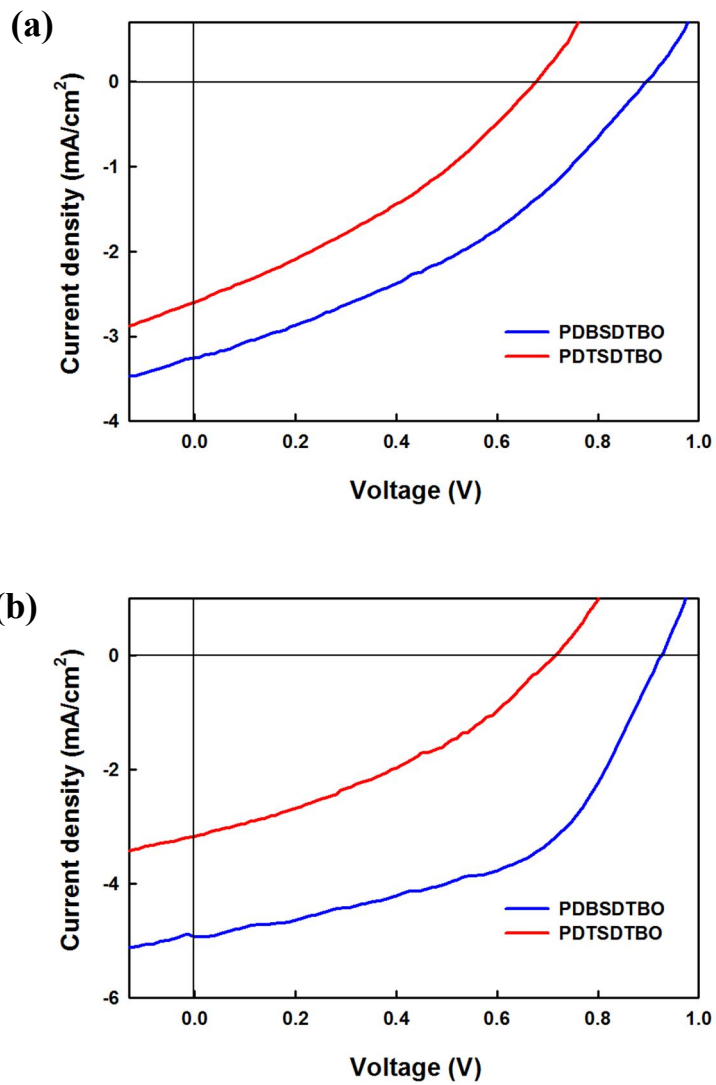


Figure 3.19 Current-voltage (J-V) characteristics of polymer:PC₇₁BM BHJ solar cells under AM 1.5 condition from (a) DCB, (b) DCB with 2 vol% of D

Table 3.2 Photovoltaic properties of devices tested under standard AM 1.5G condition

Polymer:PC ₇₁ BM (1:2) (w/w)	V _{OC} (V)	J _{SC} (mA cm ⁻²)	FF (%)	PCE (%)
PDBSDTBO	0.90	3.26	36.2	1.06
PDBSDTBO ^a	0.93	4.93	51.0	2.34
PDTSDTBO	0.68	2.60	32.9	0.58
PDTSDTBO ^a	0.72	3.17	34.6	0.79

^a Processed with 2 vol% of DIO.

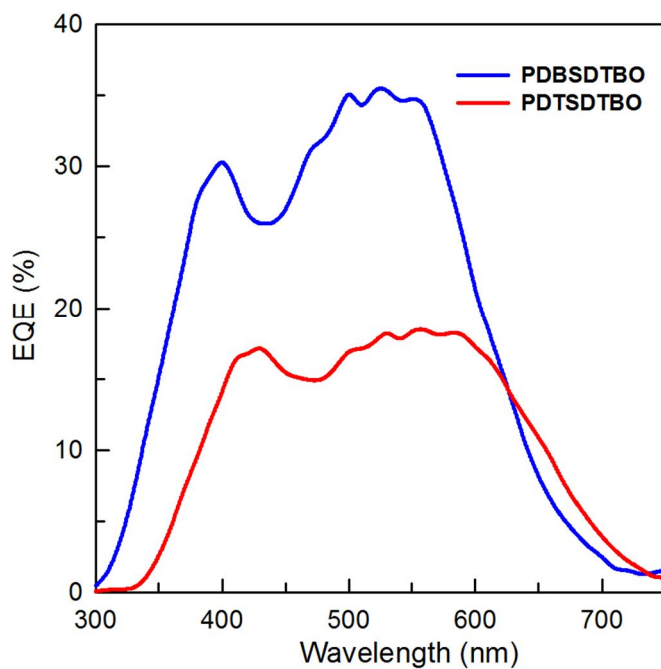


Figure3.20 External quantum efficiency spectra of polymer-PC₇₁BM solar cells processed with 2 vol% of DIO.

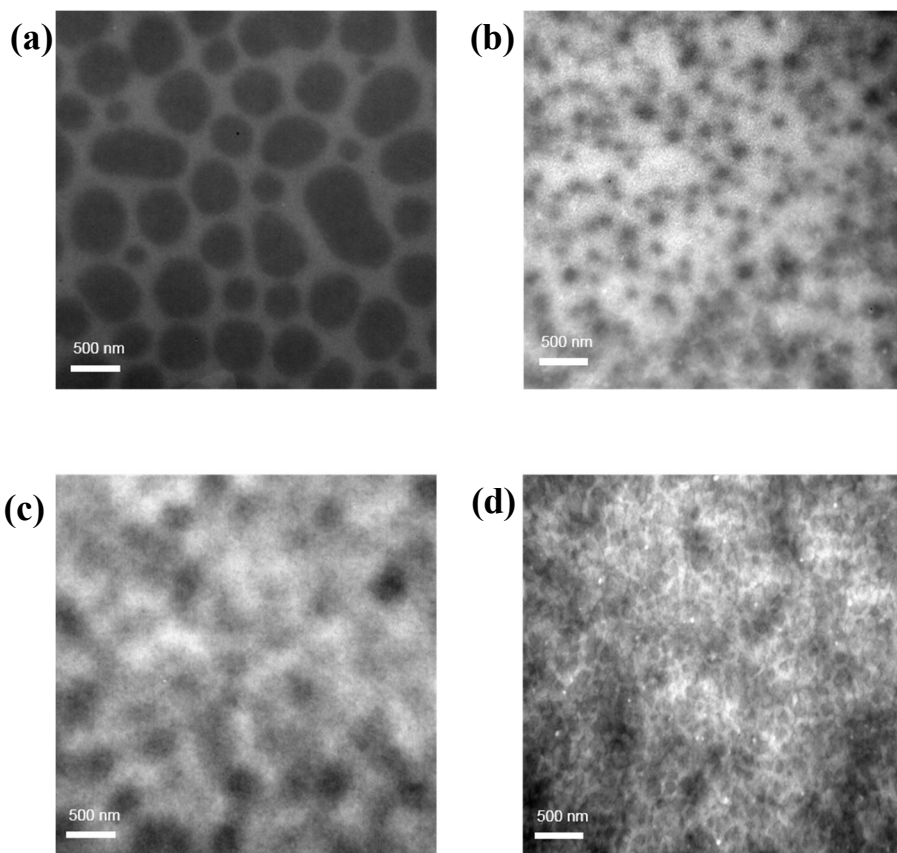


Figure 3.21 TEM images of polymer:PC₇₁BM (1:2, w/w) blend films spin-coated from DCB solution for (a) PDTSDTBO, (b) PDBSDTBO and processed with 2 vol% DIO for (c) PDTSDTBO, (d) PDBSDTBO.

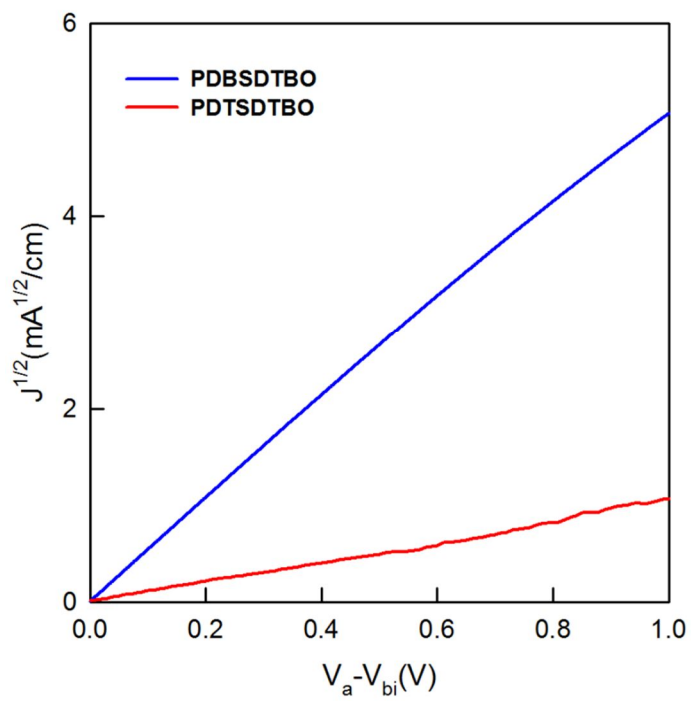


Figure3.22 Dark J-V characteristics of polymer : PC₇₁BM with hole-only devices processed with 2 vol% of DIO.

Chapter 4. Conclusions

We synthesized a D-A alternating conjugated polymer PDBSDTBO composed of electron-donating dibenzosilole (DBS) and electron-accepting benzooxadiazole(BO) by the palladium catalyzed Suzuki coupling reaction. We also prepared PDTSDTBO composed of electron-donating dithienosilole (DTS) instead of DBS as a reference. The V_{OC} of PDBSDTBO-based device (0.93 V) was higher than that of PDTSDTBO-based device (0.72 V), which is in accordance with the deeper HOMO level of the PDBSDTBO than that of PDTSDTBO. The J_{SC} and FF of PDBSDTBO-based device was also higher than that of PDTSDTBO-based device because of more light absorption of PDBSDTBO and suitable film morphology of the PDBSDTBO/PC₇₁BM blend. Consequently, the higher PCE of the PDBSDTBO-based device (2.34 %) was obtained than that of the PDTSDTBO-based device (0.79 %). This result demonstrates that the structure design weakening electron donating ability to obtain higher V_{OC} can be useful method for achieving high performance solar cells.

Bibliography

- (1)BERNARDI, J. C.*J. Chil. Chem. Soc.* **2008**, *53*, 1549.
- (2) Hoppe, H.; Sariciftci, N.S.; Meissner, D. *Mol. Cryst. Liq. Cryst.***2002**, *385*, 113.
- (3) Roncali, *J. Chem. Rev.***1997**, *97*, 173.
- (4) Dimitrakopoulos, C.D.; Malenfant, P.R.L. *Adv. Mater.***2002**, *14*, 99.
- (5) Singh, B.; Sariciftci, N. S. *Ann. Rev. Mater. Res.***2006**, *36*, 199.
- (6) Lane, P.A.; Rostalski, J.; Giebeler, C.; Martin, S. I.; Bradley, D. D. C.; Meissner, D. *Sol. Energy Mater. Sol. Cells***2000**, *63*, 3.
- (7)Lehovec, K. *Phys. Rev.* **1948**, *74*, 463.
- (8)Chapin, D. M.; Fuller, C. S.; Pearsom, G. L. *J. Appl. Phys.***1954**, *25*,676.
- (9)Spanggaard, H. ; Krebs, F.C. *Sol. Energy Mater. Sol. cells***2004**, *83*, 125.
- (10)Cheng, Y.J.; Yang, S.H.; Hsu, C. S. *Chem. Rev.* **2009**, *109*, 5868.
- (11)Hoppe, H.; Sariciftci, N. S. *J. Mater. Chem.* **2004**, *19*, 1924.
- (12)Lane, P. A.; Rostalski, J.; Giebeler, C.; Martin, S. I.; Bradley, D. D.C.; Meissner, D. *Sol. Energy Mater. Sol. Cells***2000**, *63*,3.
- (13) Sivula, K.; Luscombe, C. K.; Thompson, B.C.; Frechet, J. M. J. *J. Am. Chem. Soc.***2006**, *128*, 13988.
- (14) Hou, J.; Tan, Z.; Yan, Y.; He, Y.; Yang, C.; Li, Y. *J. Am. Chem. Soc.* **2006**, *128*, 4911.

- (15) Ballantyne, A. M.; Chen, L.; Nelson, J.; Bradley, D. D. C.; Astuti, Y.; Maurano, A.; Shuttle, C. G.; Durrant, J. R.; Heeney, M.; Duffy, W.; McCulloch, I. *Adv. Mater.* **2007**, *19*, 4544.
- (16) Wu, P.-T.; Xin, H.; Kim, F. S.; Ren, G.; Jenekhe, S. A. *Macromolecules* **2009**, *42*, 8817.
- (17) Chen, H. Y.; Hou, J. H.; Zhang, S. Q.; Liang, Y. Y.; Yang, G. W.; Yang, Y.; Yu, L. P.; Wu, Y.; Li, G. *Nat. Photon.* **2009**, *3*, 649.
- (18) Dou, L. T.; You, J. B.; Yang, J.; Chen, C. C.; He, Y. J.; Murase, S.; Moriarty, T.; Emery, K.; Li, G.; Yang, Y. *Nat. Photon.* **2012**, *6*, 180.
- (19) He, Z.; Zhong, C.; Huang, X.; Wong, W. Y.; Wu, H.; Chen, L.; Su, S.; Cao, Y. *Adv. Mater.* **2011**, *23*, 4636.
- (20) Huo, L.; Hou, J.; Zhang, S.; Chen, H. Y.; Yang, Y. *Angew. Chem., Int. Ed.* **2010**, *49*, 1500.
- (21) Song, J.; Du, C.; Li, C., Bo, J. *J. Polym. Sci. Part : Polym. Chem.* **2011**, *49*, 4267.
- (22) Chan, K. L.; McKiernan, M. J.; Towns, C. R.; Holmes, A. B. *J. Am. Chem. Soc.* **2005**, *127*, 7662–7663.
- (23) Usta, H.; Lu, G.; Facchetti, A.; Marks, T. J. *J. Am. Chem. Soc.* **2006**, *128*, 9034.
- (24) Tamao, K.; Uchida, M.; Izumizawa, T.; Furukawa, K.; Yamaguchi, S. *J. Am. Chem. Soc.* **1996**, *118*, 11974.

- (25) Zhan, X. W.; Risko, C.; Amy, F.; Chan, C.; Zhao, W.; Barlow, S.; Kahn, A.; Bredas, J. L.; Marder, S. R. *J. Am. Chem. Soc.* **2005**, *127*, 9021.
- (26) Lu, G.; Usta, H.; Risko, C.; Wang, L.; Facchetti, A.; Ratner, M.A.; Marks, T. J. *J. Am. Chem. Soc.* **2008**, *130*, 7670.
- (27) Hou, L. J.; Yu, H.; Hou, J. H.; Chen, T. L.; Yang, Y. *Chem. Commun.* **2009**, *37*, 5570.
- (28) Jiang, J.M.; Yang, P.A.; Yu, C.M.; Lin, H.K.; Huang, K.C.; Wei, K.H. *J. Polym. Sci., Part A: Polym. Chem.* **2012**, *50*, 3960.
- (29) Jiang, J. M.; Yang, P. A.; Hsieh, T. H.; Wei, K. H. *Macromolecules* **2011**, *44*, 9155
- (30) Ding, P.; Zhong, C. M.; Zou, Y.P.; Pan, C. Y.; Wu, H. B.; Cao, Y. *J. Phys. Chem. C*, **2011**, *115*, 16211.
- (31) Zhou, H. X.; Yang, L.; Stoneking, S.; You, W. *Appl. Mater. Interfaces*, **2010**, *2*, 1377.
- (32) Yuan, M. C.; Su, M. H.; Chiu, M. Y.; Wei, K. H. *J. Polym. Sci. Part A: Polym. Chem.* **2009**, *48*, 1298.
- (33) Melzer, C.; Koop, E. J.; Mihailitchi, V. D.; Blom, P. W. *Adv. Funct. Mater.* **2004**, *14*, 865.

- (34) Kline R. J.; McGehee M. D.; Kadnikova E. N.; Liu J.; Fréchet J. M. J.
Adv. Mater. **2003**, *15*, 1519.
- (35) Yang, J.; Hou, Q.; Yang, W.; Zhang, C.; Cao Y. *Macromolecules*,
2005, *38*, 244.
- (36) Kanimozhi, C.; Balraju, P.; Sharma, G. D.; Patil, S. *J. Phys. Chem. B*,
2010, *114*, 3095.
- (37) Scharber M. C.; Mühlbacher D.; Koppe M.; Denk P.; Waldauf C.;
Heeger A. J. et al. *Adv Mater*, **2006**, *18*, 789.
- (38) Zoombelt, A. P.; Fonrodona, M.; Turbiez, M. G. R.; Wienk, M. M.;
Janssen, R. A. J. *J. Mater. Chem.* **2009**, *19*, 5336.
- (39) Chiu, M. Y.; Jeng, U. S.; Su, M. S.; Wei, K. H. *Macromolecules* **2010**,
43, 428.
- (40) Kotlarski, J. D.; Moet, D. J. D.; Blom, P. W. M. *J. Polym. Sci., Part B:
Polym. Phys.* **2011**, *49*, 708–711.
- (41) Shrotriya, V.; Wu, E. H.-E.; Li, G.; Yao, Y.; Yang, Y. *Appl. Phys.
Lett.* **2006**, *88*, 064104.

초 록

본 연구에서는 유기태양전지에 사용되는 dibenzosilole(DBS)과 benzooxadiazole(BO)로 이루어진 D-A 전도성 고분자 PDBSDTBO를 palladium 촉매를 사용한 Suzuki coupling에 의해 합성하였다. 이는 최근 관심 받는 전자주개인 dithienosilole (DTS)의 단점인 낮은 HOMO에너지 레벨로 인한 낮은 개방전압을 향상시키기 위해서 dithienosilole의 thiophene부분을 전자주개능력이 약한 벤젠으로 치환하여 HOMO 에너지 레벨을 낮추고 그에 따른 전압 향상 및 효율 향상에 그 목적이 있다. PDBSDTBO 고분자의 광학적질을 분석한 결과 660 nm까지 광흡수를 하여 밴드갭이 1.88 eV를 나타내었고, 전기화학적 성질을 분석한 결과 HOMO 에너지레벨이 -5.52 eV로 DTS를 기반으로 하는 고분자 PDTSDTBO보다 약 0.2eV 낮음을 확인하였다. 합성된 고분자를 PC₇₁BM 과 블렌딩을 하여 제작한 유기태양전지소자의 경우, DTS를 기반으로하는 고분자와 비교하였을때, 개방전압이 0.93 V으로 DTS의 경우보다 0.2 V높았으며, 단락전류와 FF의 경우에도 각각 상승하여 전체적으로 약 2.34%에 해당하는 더 높은 효율을 얻을 수 있다.

주요어: Benzo[c][1,2,5]oxadiazole, 전도성고분자, 높은개방전압,

Dibenzosilole, 유기태양전지

학번: 2012-22542